A SIMPLE, ACCURATE WALL LOSS FILTER FOR ACOUSTIC TUBES

Jonathan Abel

Universal Audio
Santa Cruz, CA 94060, USA
abel@uaudio.com

Tamara Smyth and Julius O. Smith III

CCRMA, Stanford University
Stanford, CA 94305, USA
tamara/jos@ccrma.stanford.edu

ABSTRACT

This research presents a uniform approximation to the formulas of Benade and Keefe for the propagation constant of a cylindrical tube, valid for all tube radii and frequencies in the audio range. Based on this approximation, a simple expression is presented for a filter which closely matches the thermoviscous loss filter of a tube of specified length and radius at a given sampling rate. The form of this filter and the simplicity of coefficient calculation make it particularly suitable for real-time music applications where it may be desirable to have tube parameters such as length and radius vary during performance.

1. INTRODUCTION

In practical implementations of acoustic tubes using digital waveguide synthesis, it is necessary to account for the losses associated with viscous drag and thermal conduction which take place primarily within a thin boundary layer along the bore walls [1, pp. 127–129]. Though these losses are *distributed* over the length of the tube, in a digital waveguide implementation it is more efficient to lump these effects by *commuting* a characteristic digital filter to each end of the waveguide (and any intervening observation points) [2, 3], as illustrated in Figure 1.

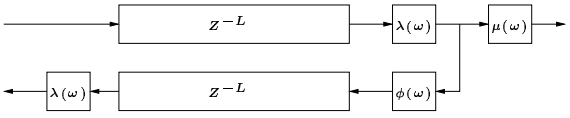

Figure 1: *A waveguide model of a cylindrical tube with commuted wall loss filters, $\lambda(\omega)$, at upper and lower delay line observation points, a reflection filter $\phi(\omega)$ and a transmission filter $\mu(\lambda)$.*

In [4] Benade gives formulas for calculating the propagation constant in a cylindrical tube of arbitrary radius, and presents simple approximations, valid for either low frequencies (and/or small tubes) or high frequencies (and/or large tubes). Later Keefe [5] presents separate higher-order approximations for large and small tubes. The propagation constant gives the phase velocity and the attenuation coefficient necessary for designing the loss filter $\lambda(\omega)$ which is commonly derived using the large tube approximation [1, pp. 27–29].

In this work we present a uniform approximation to the attenuation and phase velocity models of Benade and Keefe. Based on this uniform approximation we observe that the loss filter is minimum phase and evaluate several minimum phase filter design methods, including a cascade of first-order shelf filters with parameters specified by simple functions of tube radius, tube length, and sampling rate. All filter design methods have comparable accuracy for a given order of digital filter, while the shelf filter cascade has the advantage of design simplicity and is nicely parameterized for time varying tube geometries.

2. THERMOVISCOUS LOSSES IN CYLINDRICAL CONDUITS

In a cylindrical conduit, the walls contribute a viscous drag dependent on the ratio of the pipe radius a to the thickness of the viscous boundary layer given by the parameter

$$r_v = a\left(\frac{\eta}{\omega\rho}\right)^{-\frac{1}{2}}, \tag{1}$$

where ρ is the density of air, η is the viscosity and ω the radian frequency [6, pp. 193–196].

Further losses may occur due to a thermal exchange between the air and the walls with a magnitude dependent on the ratio of the tube radius a to the thermal boundary layer thickness given by the parameter

$$r_t = a\left(\frac{\kappa}{\omega\rho C_p}\right)^{-\frac{1}{2}}, \tag{2}$$

where κ is the thermal conductivity and C_p is the specific heat of air at constant pressure [6, pp. 193–196]. The two ratios are related by the square root of the Prandtl number ν^2 [4], that is,

$$r_t = \nu r_v, \qquad \nu = [C_p\eta/\kappa]^{\frac{1}{2}}. \tag{3}$$

Values for gas constants for air are given in Table 1.

The effects of the viscous and thermal losses lead to an attenuation in the waves propagating down the length of the pipe. The propagation constant is given by

$$\Gamma(\omega) = \alpha(\omega) + j\frac{\omega}{v(\omega)}, \tag{4}$$

where $\alpha(\omega)$ is the attenuation coefficient, ω is the radian frequency and $v(\omega)$ is the phase velocity of wave disturbances [4].

Benade gives the following approximations for both the phase velocity $v(\omega)$ and the attenuation coefficient $\alpha(\omega)$ in the limit of small and large tube radius boundary-layer thickness ratios [4]:

$$v(\omega) = \begin{cases} c\dfrac{r_v}{2\sqrt{\gamma}}, & r_v \ll 1 \\ c\left[1 - \dfrac{1}{r_v\sqrt{2}}\left(1 + \dfrac{(\gamma-1)}{\nu}\right)\right], & r_v \gg 1 \end{cases} \tag{5}$$

$$\alpha(\omega) = \begin{cases} \left(\frac{\omega}{c}\right)\frac{2\sqrt{\gamma}}{r_v}, & r_v \ll 1 \\ \left(\frac{\omega}{c}\right)\frac{1}{r_v\sqrt{2}}\left(1+\frac{(\gamma-1)}{\nu}\right), & r_v \gg 1. \end{cases} \tag{6}$$

Constant	Symbol	Value	Unit
air density	ρ	1.18×10^{-3}	g/cm^2
viscosity	η	1.85×10^{-4}	$g/(s \times cm)$
Prandtl	ν^2	0.841	
ratio of specific heats	$\gamma = C_p/C_v$	1.40	
free space sound speed	c	3.47×10^4	cm/s

Table 1: *Gas constants for air evaluated at* $26.86C$.

It is possible to account for attenuation due to wall losses simply by multiplying delay line outputs by a single coefficient β [7, page 466]. For a tube of length L and radius a, with observation points at the ends of the upper and lower delay lines, the constant β has the following approximate value:

$$\beta \approx 1 - 2\alpha L, \qquad \alpha \approx 2 \times 10^{-5}\omega^{\frac{1}{2}}/a, \tag{7}$$

where the approximation is valid for tubes sufficiently short that β is near one.

Since losses are frequency dependent, this coefficient is only a rough estimate. In practice, the simple large r_v expressions are commonly used to design wall loss filters for musical wind instrument physical models (see, e.g. [1, page 129]) and given the relatively large bores of most instruments, this is likely an acceptable approximation. These expressions may not, however, be sufficiently accurate for smaller tubes like those found in some biological sound production mechanisms such as the bronchi and trachea in birds [8]. Therefore, in order to have a more versatile acoustic tube model, it is preferable for the wall loss filter to make use of a single less restrictive expression for phase velocity and attenuation—one that is compatible with all tube sizes and frequencies.

3. A UNIFORM APPROXIMATION FOR PHASE VELOCITY AND ATTENUATION

The asymptotic behavior of phase velocity and attenuation for large and small r_v is given by (5) and (6). The following single expression is a uniform approximation for the phase velocity, valid for any r_v:

$$v(\omega) = c\,\frac{A_v r_v(1 + r_v/k)}{1 + A_v r_v(B_v + r_v/k)}, \tag{8}$$

where the parameters A_v and B_v, given by

$$A_v = \frac{1}{2\sqrt{\gamma}}, \qquad B_v = 1 + \frac{[1 + (\gamma-1)/\nu)]}{\sqrt{2}k}, \tag{9}$$

were selected to match the limiting phase velocity behavior and the parameter

$$k = 2\gamma \tag{10}$$

marks the ratio r_v delimiting the small and large tube regions.

Similarly a uniform approximation for the attenuation coefficient is

$$\alpha(\omega) = \left(\frac{\omega}{cr_v}\right)\frac{A_\alpha + B_\alpha\,(r_v/k)}{1 + r_v/k}, \tag{11}$$

where the parameters A_α and B_α were again selected to match the limiting attenuation coefficient behavior and are given by

$$A_\alpha = 2\sqrt{\gamma}, \qquad B_\alpha = \frac{[1 + (\gamma-1)/\nu]}{\sqrt{2}}. \tag{12}$$

Figures 2 and 3 show the uniform approximations for phase velocity and attenuation along with their limiting behaviors.

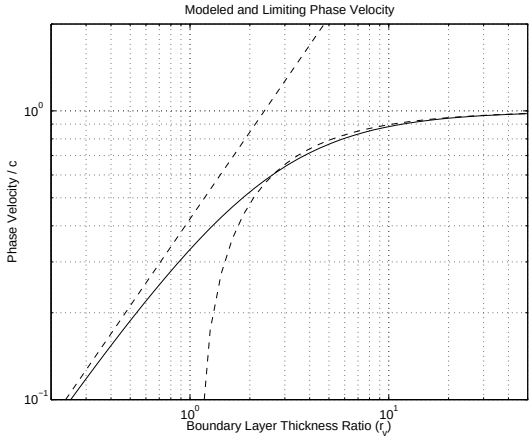

Figure 2: *Modeled uniform phase velocity (solid) and the limiting behavior (dashed).*

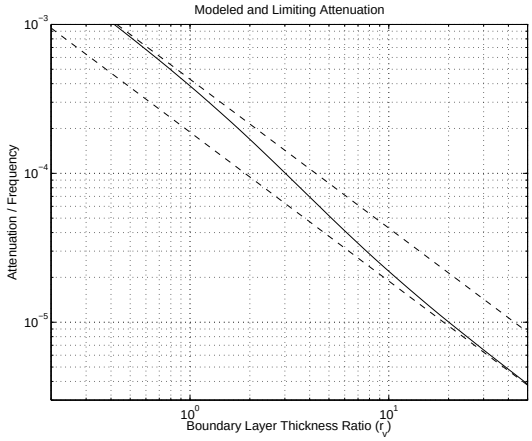

Figure 3: *Modeled uniform attenuation (solid) and the limiting behavior (dashed).*

4. WALL LOSS FILTER

4.1. Filter Characteristic

The propagation constant $\Gamma(\omega)$ in (4) gives the per unit length attenuation of waves propagating along an infinitely long tube act-

ing as a transmission line. Accordingly, the following frequency response approximates the attenuation and phase delay over a tube of length L:

$$e^{-\Gamma(\omega)L} = e^{-\alpha(\omega)L - j(\omega/v(\omega))L}. \quad (13)$$

Removing a pure delay of duration L/c, we have the desired wall loss filter frequency response $\lambda(\omega)$, given by

$$\lambda(\omega) = e^{-\alpha(\omega)L - j(\omega/v(\omega) - \omega/c)L}. \quad (14)$$

Noting that the attenuation $\alpha(\omega)$ increases with the square root of frequency, the wall loss filter $\lambda(\omega)$ is seen to have a gentle low-pass characteristic. This low-pass characteristic is more pronounced with decreasing tube radius a or increasing tube length L, as illustrated in Figures 4 and 5 respectively.

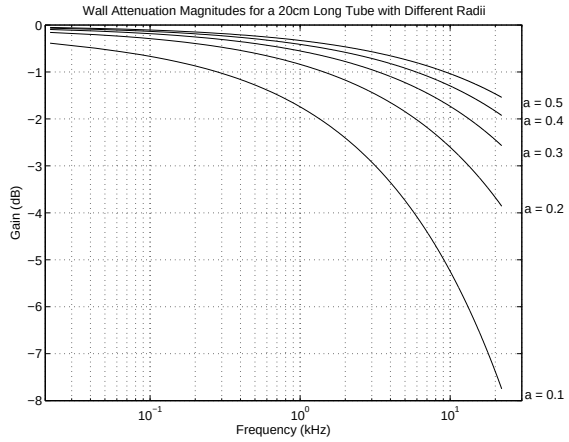

Figure 4: *Wall loss filter magnitude $|\lambda(\omega)|$, showing a low-pass characteristic that is more pronounced with a decreasing tube radius (radius values, a, given in cm).*

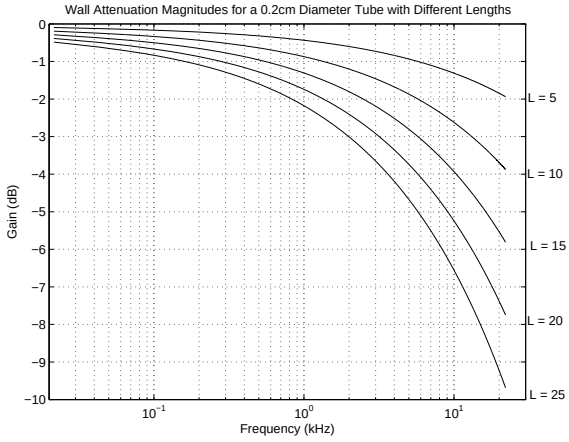

Figure 5: *Wall loss filter magnitude $|\lambda(\omega)|$, showing a low-pass characteristic that is more pronounced with an increasing tube length (length values, L, given in cm).*

While not yet confirmed analytically, numerical results indicate that the wall loss filter $\lambda(\omega)$ is minimum phase. In the sequel, we assume this property holds, and consider only those design methods which produce minimum phase filters.

4.2. Filter Design

Given the desired wall loss filter transfer function $\lambda(\omega)$ expressed in terms of the tube parameters and physical constants, what remains is to compute the coefficients of a digital filter approximating the desired transfer function for frequencies up to the Nyquist limit. The wall loss magnitude is a relatively smooth function of frequency, and computationally efficient low-order rational filters are expected to provide a good fit.

Warped Prony [9] and Hankel norm methods [10] were used to fit low-order rational filters to $\lambda(\omega)$. While the fit to the attenuation filter is good, as shown in the examples of Figures 6 and 7, these methods require considerable computation and are not convenient for a filter based on tube parameters likely to change in real-time. Additionally, in settings where tube parameters are time varying, the fit may produce real poles for some parameter values and complex poles for other making it difficult to smoothly transition between wall loss filters.

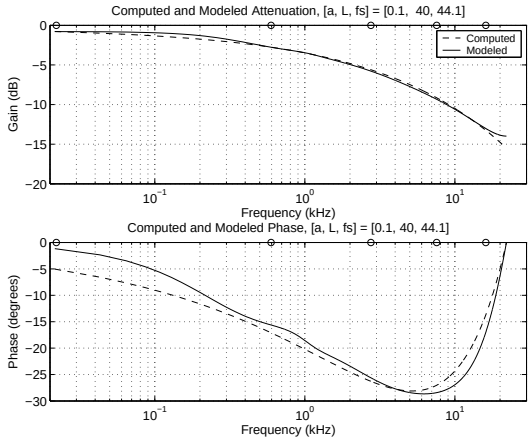

Figure 6: *Warped Prony fifth-order model and computed wall loss filter transfer functions illustrating an excellent fit at all frequencies.*

To circumvent problems with standard modeling techniques, consider a cascade of minimum-phase first-order shelf filters $\sigma_i(z)$ [11],

$$\hat{\lambda}(z) = \prod_{i=1}^{N} \sigma_i(z; f_t(i), g_\pi(i)), \quad (15)$$

with each shelf filter having a DC gain of one, a band edge gain $g_\pi(i)$, and a gain $\sqrt{g_\pi(i)}$ at its transition frequency $f_t(i)$. As shown in the Appendix, the shelf filter coefficients are easily computed in real time. Also, since the shelf filters are first order, they have real poles and zeros, and are relatively free of artifacts when made time varying.

First-order shelf filters have transfer functions which slowly transition between their DC and band edge values. It therefore seems reasonable that a cascade of shelf filters with judiciously chosen transition frequencies and gains could approximate the desired wall loss transfer function.

As seen in Figures 4 and 5, the desired wall loss filters as a function of tube length, radii, and sampling rate are strikingly self

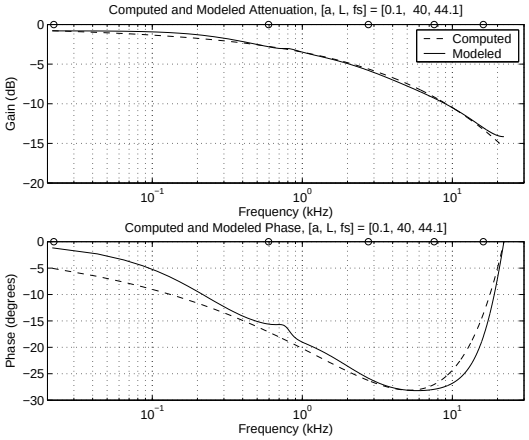

Figure 7: *Hankel norm fifth-order model and computed wall loss filter transfer functions illustrating an excellent fit at all frequencies.*

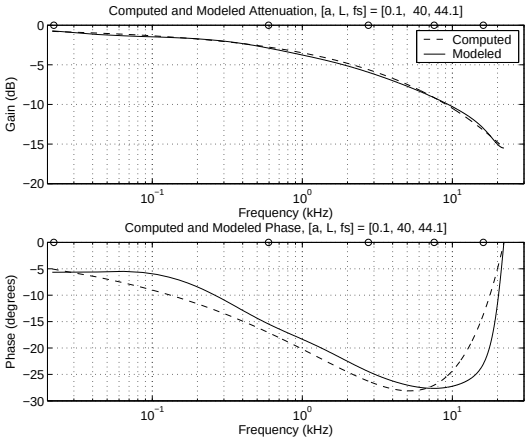

Figure 8: *Computed and modeled wall loss filter illustrating an excellent fit at all frequencies using a cascade of first-order filters to produce a fifth-order IIR filter.*

similar under the appropriate stretching of the log magnitude or frequency axes. Initially, the idea was to design via brute-force optimization a low-order shelf filter cascade which matched the desired transfer function at a particular sampling rate and tube geometry. This prototype filter could then be stretched in response to sampling rate and conduit geometry.

In designing the prototype filters for different orders however, a pattern emerged and we discovered that the cascade of shelf filters with band-edge gains (in units of amplitude) and transition frequencies (in radians/π) given by

$$\begin{aligned} g_\pi(i) &= \exp\left\{ \frac{[(i-\frac{1}{2})/N]^{\frac{1}{2}}}{\sum_{k=1}^{N}[(k-\frac{1}{2})/N]^{\frac{1}{2}}} \cdot \ln|\lambda(2\pi f_s/2)| \right\}, \\ f_t(i) &= \left[(i-\frac{1}{2})/N\right]^3, \end{aligned} \tag{16}$$

has a transfer function which, as illustrated in Figures 9–11, is an excellent approximation to $\lambda(\omega)$ for a wide range of filter orders N, tube lengths L, tube radii a, and sampling rates f_s.

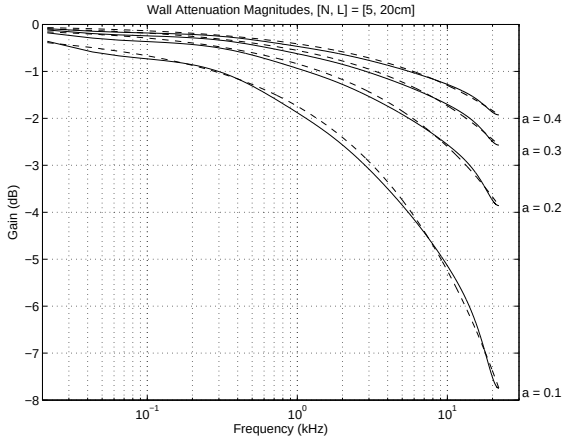

Figure 9: *Computed and shelf filter cascade wall loss filter magnitude at various tube radii (values given in cm) with the filter order, N, and the tube length, L, constant.*

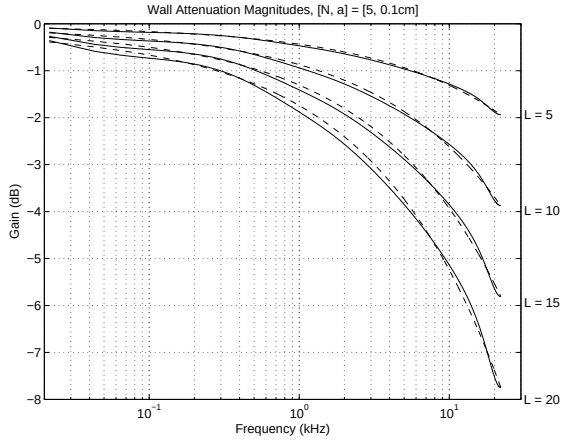

Figure 10: *Computed and shelf filter cascade wall loss filter magnitude at various tube lengths (values given in cm) with the filter order, N, and the tube radius, a, constant.*

In the presence of a changing tube geometry, we recommend that the filter $\hat{\lambda}(z)$ be implemented as a cascade of first-order sections, with coefficients linearly or exponentially interpolated between computed values. In this way, the dynamic range of the filter coefficients is minimized, and filters having interpolated coefficients are guaranteed to be stable with transfer functions roughly matching those associated with intermediate values of geometric parameters. Note that fifth-order filters are sufficient to give transfer functions accurate to withing a fraction of a dB across the audio band for typical audio sampling rates.

5. CONCLUSIONS

Wall attenuation filters are an important part of acoustic tube models (used by a large body of musical instruments) and should not

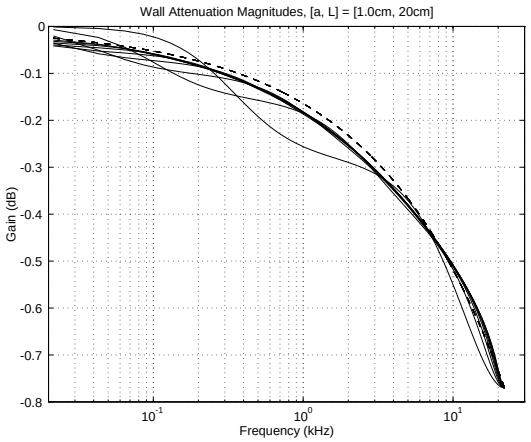

Figure 11: *Computed and shelf filter cascade wall loss filter magnitude using* $2, 3, \ldots, 10$ *first-order shelf filters.*

be neglected for the sake of simplicity. Though their audibility may be slight for certain tube geometries, they can contribute significantly to the reduction of high frequency components that lead to aliasing and can also eliminate some sources of instability in the model. Though approximations will often be satisfactory, it is worthwhile to aim for a more robust, scientifically sound and versatile solution.

As exemplified by Figures 9–11, a cascade of first-order shelf filters provides an excellent approximation to the cylindrical tube wall loss transfer function $\lambda(\omega)$ for a wide range of filter orders, tube lengths, tube radii, and sampling rates. It is also efficient to compute for continually changing parameters making it an ideal choice for modeling wall losses in acoustic tubes.

6. APPENDIX: FIRST-ORDER SHELF FILTER COEFFICIENT COMPUTATION

This appendix presents formulas for computing the coefficients of the first-order shelf filters used above.

The transfer function for the first-order shelf filter is given by

$$\sigma(z; f_t, g_\pi) = \frac{b_0 + b_1 z^{-1}}{1 + a_1 z^{-1}}. \tag{17}$$

Having unity gain at DC, a band edge gain $g_\pi \geq 0$ (the gain at the Nyquist limit) and a gain $\sqrt{g_\pi}$ at the transition frequency f_t measured in radians$/\pi$, the coefficients in (17) are given by

$$b_0 = \frac{\beta_0 + \rho\beta_1}{1 + \rho\alpha_1}, \tag{18}$$

$$b_1 = \frac{\beta_1 + \rho\beta_0}{1 + \rho\alpha_1}, \tag{19}$$

$$a_1 = \frac{\rho + \alpha_1}{1 + \rho\alpha_1}, \tag{20}$$

where

$$\beta_0 = (1 + g_\pi)/2 + (1 - g_\pi)\alpha_1/2, \tag{21}$$

$$\beta_1 = (1 - g_\pi)/2 + (1 + g_\pi)\alpha_1/2, \tag{22}$$

and

$$\alpha_1 = \begin{cases} 0, & g_\pi = 1 \\ \eta - \mathrm{sign}(\eta)(\eta^2 - 1)^{\frac{1}{2}}, & g_\pi \neq 1. \end{cases} \tag{23}$$

To form the coefficients of a prototype shelf filter with a transition frequency of $\pi/2$, η from (23) is set to the following:

$$\eta = (g_\pi + 1)/(g_\pi - 1), \quad g_\pi \neq 1. \tag{24}$$

The parameter

$$\rho = \sin(\pi f_t/2 - \pi/4)/\sin(\pi f_t/2 + \pi/4) \tag{25}$$

is the coefficient of the first-order allpass transformation warping the prototype filter to the proper transition frequency.

7. REFERENCES

[1] Gary Paul Scavone, *An Acoustic Analysis of Single-Reed Woodwind Instruments with an Emphasis on Design and Performance Issues and Digital Waveguide Modeling Techniques*, Ph.D. thesis, CCRMA, Music Dept., Stanford University, Stanford, California, March 1997, available as CCRMA Technical Report No. STAN–M–100 or from ftp://ccrma-ftp.stanford.edu/pub/Publications/Theses/-GaryScavoneThesis/.

[2] Julius O. Smith, "Physical modeling using digital waveguides," *Computer Music Journal*, vol. 16, no. 4, pp. 74–91, 1992, Special issue: Physical Modeling of Musical Instruments, Part I.

[3] Julius O. Smith, *Digital Waveguide Modeling of Musical Instruments*, www-ccrma.stanford.edu/~jos/waveguide/, 2003.

[4] A. H. Benade, "On the propagation of sound waves in a cylindrical conduit," *Joural of the Acoustical Society of America*, vol. 44, no. 2, pp. 616–623, 1968.

[5] D. H. Keefe, "Acoustical wave propagation in cylindrical ducts: Transmission line approximation for isothermal and nonisothermal boundary conditions," *Joural of the Acoustical Society of America*, vol. 75, no. 1, pp. 58–62, Januaray 1984.

[6] Neville H. Fletcher and Thomas D. Rossing, *The Physics of Musical Instruments*, Springer-Verlag, 1995.

[7] Neville H. Fletcher, "Bird song – a quantitative acoustic model," *Journal of Theoretical Biology*, vol. 135, pp. 455–481, 1988.

[8] Tamara Smyth and Julius O. Smith, "The syrinx: Nature's hybrid wind instrument," in *CD-ROM Paper Collection*, Cancun Mexico, September 2002, Pan-America/Iberian Meeting on Acoustics.

[9] Julius O. Smith and Jonathan S. Abel, "Bark and ERB bilinear transforms," *IEEE Transactions on Speech and Audio Processing*, November 1999.

[10] Julius Smith, *Techniques for Digital Filter Design and System Identification with Applications to the Violin*, Ph.D. thesis, Stanford University, Stanford, California, June 1983.

[11] Udo Zölzer, *Digital Audio Signal Processing*, John Wiley and Sons, Inc., New York, 1999.